

<https://doi.org/10.3348/kjr.2017.18.4.585>

pISSN 1229-6929 · eISSN 2005-8330

Korean J Radiol 2017;18(4):585-596



# Influence of $B_1$ -Inhomogeneity on Pharmacokinetic Modeling of Dynamic Contrast-Enhanced MRI: A Simulation Study

Bumwoo Park, BE<sup>1, 2\*</sup>, Byung Se Choi, MD<sup>3\*</sup>, Yu Sub Sung, PhD<sup>1, 2</sup>, Dong-Cheol Woo, PhD<sup>1, 2</sup>, Woo Hyun Shim, PhD<sup>1, 2</sup>, Kyung Won Kim, MD<sup>1, 2</sup>, Yoon Seok Choi, PhD<sup>1, 2</sup>, Sang Joon Pae, MD<sup>4</sup>, Ji-Yeon Suh, PhD<sup>1, 2</sup>, Hyungjoon Cho, PhD<sup>5</sup>, Jeong Kon Kim, MD<sup>1, 2</sup>

<sup>1</sup>Department of Radiology, Research Institute of Radiology, Asan Medical Center, University of Ulsan College of Medicine, Seoul 05505, Korea;

<sup>2</sup>Center for Bioimaging of New Drug Development, Asan Institute for Life Sciences, Asan Medical Center, University of Ulsan College of Medicine, Seoul 05505, Korea; <sup>3</sup>Department of Radiology, Seoul National University College of Medicine, Seoul National University Bundang Hospital, Seongnam 13620, Korea; <sup>4</sup>Department of Surgery, National Health Insurance Service Ilsan Hospital, Goyang 10444, Korea; <sup>5</sup>Biomedical Engineering, Ulsan National Institute of Science and Technology, Ulsan 44919, Korea

**Objective:** To simulate the  $B_1$ -inhomogeneity-induced variation of pharmacokinetic parameters on dynamic contrast-enhanced magnetic resonance imaging (DCE-MRI).

**Materials and Methods:**  $B_1$ -inhomogeneity-induced flip angle (FA) variation was estimated in a phantom study. Monte Carlo simulation was performed to assess the FA-deviation-induced measurement error of the pre-contrast  $R_1$ , contrast-enhancement ratio, Gd-concentration, and two-compartment pharmacokinetic parameters ( $K^{\text{trans}}$ ,  $v_e$ , and  $v_p$ ).

**Results:**  $B_1$ -inhomogeneity resulted in -23–5% fluctuations (95% confidence interval [CI] of % error) of FA. The 95% CIs of FA-dependent % errors in the gray matter and blood were as follows: -16.7–61.8% and -16.7–61.8% for the pre-contrast  $R_1$ , -1.0–0.3% and -5.2–1.3% for the contrast-enhancement ratio, and -14.2–58.1% and -14.1–57.8% for the Gd-concentration, respectively. These resulted in -43.1–48.4% error for  $K^{\text{trans}}$ , -32.3–48.6% error for the  $v_e$ , and -43.2–48.6% error for  $v_p$ . The pre-contrast  $R_1$  was more vulnerable to FA error than the contrast-enhancement ratio, and was therefore a significant cause of the Gd-concentration error. For example, a -10% FA error led to a 23.6% deviation in the pre-contrast  $R_1$ , -0.4% in the contrast-enhancement ratio, and 23.6% in the Gd-concentration. In a simulated condition with a 3% FA error in a target lesion and a -10% FA error in a feeding vessel, the % errors of the pharmacokinetic parameters were -23.7% for  $K^{\text{trans}}$ , -23.7% for  $v_e$ , and -23.7% for  $v_p$ .

**Conclusion:** Even a small degree of  $B_1$ -inhomogeneity can cause a significant error in the measurement of pharmacokinetic parameters on DCE-MRI, while the vulnerability of the pre-contrast  $R_1$  calculations to FA deviations is a significant cause of the miscalculation.

**Keywords:** Brain; Magnetic resonance imaging; Dynamic contrast enhancement; Monte Carlo method; Phantoms, imaging

Received August 16, 2016; accepted after revision November 18, 2016.

This work was supported by Basic Science Research Program through the National Research Foundation of Korea (NRF) funded by the Ministry of Education, Science and Technology (2011-0028826) and by a grant of the Korea Health Technology R&D Project through the Korea Health Industry Development Institute (KHIDI), funded by the Ministry of Health & Welfare, Republic of Korea (grant number: HI14C1090).

\*These authors contributed equally to this work.

**Corresponding author:** Jeong Kon Kim, MD, Department of Radiology, Research Institute of Radiology, Asan Medical Center, University of Ulsan College of Medicine, 88 Olympic-ro 43-gil, Songpa-gu, Seoul 05505, Korea.

• Tel: (822) 3010-5981 • Fax: (822) 3010-0090 • E-mail: Email: kim.jeongkon@gmail.com

This is an Open Access article distributed under the terms of the Creative Commons Attribution Non-Commercial License (<http://creativecommons.org/licenses/by-nc/4.0>) which permits unrestricted non-commercial use, distribution, and reproduction in any medium, provided the original work is properly cited.

## INTRODUCTION

Dynamic contrast-enhanced magnetic resonance imaging (DCE-MRI) is considered a useful tool for evaluating angiogenic alterations in various disease entities. As an advanced analysis technique, pharmacokinetic (PK)-modeling on DCE-MRI can quantify the functional status of vessels, such as transvascular permeability and blood volume. Given this advantage, PK parameters using DCE-MRI are predicted to be promising biomarkers for assessing the response to antiangiogenic treatment (1-3).

In order to accept the DCE-MRI-derived PK parameters as relevant indicators for predicting treatment response and patient prognosis, their measurement accuracy and reliability must necessarily be satisfied. In this regard, some steps in PK modeling have potential risks for significant misestimating (4). In particular, flip angle (FA) deviation due to a defectively transmitted radiofrequency field results in incorrect quantifications of the pre-contrast  $R_1$  and the Gd-driven contrast enhancement ratio (CER). As these two values are crucial elements in converting the DCE-MRI signal to the Gd-concentration for PK modeling (5-8), such miscalculation eventually leads to inaccurate and non-reproducible estimation of PK parameters (7, 9-11).

Such unfavorable influence of  $B_1$ -inhomogeneity on PK modeling of DCE-MRI has been demonstrated in many reports (5-8). However, the degree of error propagation led by the FA fluctuation in each modeling step has not been evaluated. This detailed information is important for establishing a strategy to minimize the measurement error and for understating the principle of error transfer and/or augmentation between the PK modeling processes. From this perspective, this study was conducted to investigate the actual range of  $B_1$ -inhomogeneity and its impact on each computational process in PK modeling. Specifically, real FA variation measured on a clinical 3T MRI unit is applied to the Monte Carlo simulation that describes the  $B_1$ -dependent, erroneous PK parameter estimation. Additionally, the extent of FA inhomogeneity is measured in normal volunteers in order to predict the FA-error-induced inaccuracy of PK parameters in clinical situations. Finally, the strategy to reduce such undesirable effects of  $B_1$ -inhomogeneity on PK modeling is discussed.

## MATERIALS AND METHODS

### Measurement of *Ex Vivo* and *In Vivo* $B_1$ Error

All scans were performed on a Philips Achieva (*ex vivo*) and Ingenia (*in vivo*) 3T TX scanner (Philips Healthcare, Best, the Netherlands) that are used clinically and undergo regular equipment maintenance according to the vendor's guidelines. The  $B_1$  transmission field was evaluated in a water phantom and in the brains of three normal volunteers, using a brain coil. The 'actual flip angle imaging' method, which uses two identical radiofrequency pulses with two different repetition times ( $TR_1 < TR_2$ ) (12) was employed for measuring the  $B_1$ -inhomogeneity. The steady-state gradient echo images were obtained according to the following parameters:  $TR_1 = 30$  ms,  $TR_2 = 100$  ms, echo time (TE) = 3.74 ms, FA = 30, field of view = 200 x 200, and slice thickness = 5 mm in *ex vivo* experiments; and  $TR_1 = 30$  ms,  $TR_2 = 120$  ms, TE = 2.2 ms, FA = 30, field of view = 230 x 180, and slice thickness = 5 mm in *in vivo* experiments. A FA map was then generated from these images, and the actual FA values were measured across the midline of the phantom and the brain. Finally, the means  $\pm$  standard deviation (SD) and 95% confidence interval (CI), i.e., means  $\pm$  1.96 SD, of the actual FA were calculated.

### Monte Carlo Simulation

From the 95% CI of actual FAs measured in the phantom study, 100000 FAs were randomly extracted with the assumption of their Gaussian distribution. These FAs were then applied to measure the actual values of the pre-contrast  $R_1$  value, Gd-driven CER and the time-dependent Gd-concentration in the gray matter and blood. The  $B_1$ -dependent fluctuation of these values resulted in an incorrect estimation of the arterial input function (AIF) and the PK parameters, while the Levenberg-Marquardt method was used for fitting the time-Gd-concentration curve (13). All simulations were performed using MATLAB-based in-house software (The MathWorks, Natick, MA, USA).

For quantifying the  $B_1$ -dependent error, the % error was calculated using the following equation:

$$\% \text{ error} = \frac{\text{Actual value} - \text{nominal (reference) value}}{\text{Nominal (reference) value}} \times 100 \quad (1)$$

### Pre-Contrast $R_1$ Measurement

Flip angle-error-driven actual pre-contrast  $R_1$  values

for gray matter (reference value, 0.606 sec<sup>-1</sup>) and blood (reference value, 0.549 sec<sup>-1</sup>) were simulated using the variable flip angle (VFA) method (4, 14). For measuring the actual R<sub>1</sub>, two actual FAs corresponding to two nominal FAs of 2° and 14° were used by referring to the Quantitative Imaging Biomarker Alliance (QIBA) guidelines (15, 16).

The actual MR signal intensity (SI) determined by an erroneous FA was calculated as follows:

$$SI_a = M_0 \cdot \sin \alpha_a \cdot \frac{1 - e^{-TR \cdot R_1}}{1 - \cos \alpha_a \cdot e^{-TR \cdot R_1}} \quad (2),$$

where SI<sub>a</sub> = FA-error-dependent actual SI, M<sub>0</sub> = proton density, α<sub>a</sub> = actual FA corresponding to the nominal FA of 2° and 14°, R<sub>1</sub> = reference values of longitudinal relaxation rate (1 / T<sub>1</sub>) of gray matter and blood, and TR (2.5 msec). The actual R<sub>1</sub> value was then calculated according to the following equations (17):

$$SI_a / \sin (\alpha_n) = m \cdot SI_a / \tan (\alpha_n) + M_0 (1 - m) \quad (3),$$

$$e^{-R_1 \cdot TR} = m \quad (4),$$

where SI<sub>a</sub> = FA-error-dependent actual SI, α<sub>n</sub> is nominal FA, and TR (2.5 msec).

### Gd-Driven CER

Gd-enhanced SI at a certain time-dependent Gd-concentration was calculated according to the following equation:

$$S(t) = M_0 \cdot \sin \alpha \cdot \frac{1 - e^{-TR \cdot (R_1 + r_1 \cdot C_n(t))}}{1 - \cos \alpha \cdot e^{-TR \cdot (R_1 + r_1 \cdot C_n(t))}} \quad (5),$$

where S(t) = Gd-enhanced, time-dependent SI, M<sub>0</sub> = proton density (10000), R<sub>1</sub> = pre-contrast R<sub>1</sub> in the gray matter and blood, r<sub>1</sub> = relaxivity of the Gd-based contrast agent (3.77 sec<sup>-1</sup> mM<sup>-1</sup>), α = FA, C<sub>n</sub>(t) = reference value of the time-dependent Gd-concentration. The C<sub>n</sub>(t) was calculated according to the modified Tofts two-compartment model with reference parameter values as described in Eq-12, in which a<sub>1</sub> = 3.99 kg/L, a<sub>2</sub> = 4.78 kg/L, m<sub>1</sub> = 0.144 min<sup>-1</sup>, m<sub>2</sub> = 0.0111 min<sup>-1</sup>, D = 0.25 mM/kg, K<sup>trans</sup> = 0.05 min<sup>-1</sup>, v<sub>e</sub> = 0.21, and v<sub>p</sub> = 0.01 (6, 18, 19). In this computation, a TR of 2.5 msec and FA of 30° were applied by referring to the QIBA guidelines (16). An actual S(t) affected by the FA error was calculated by applying the actual FA and pre-

contrast R<sub>1</sub>, which were presented as ranges at each time point. In contrast, the nominal S(t) was also computed from the reference FA and pre-contrast R<sub>1</sub>. Consequently, the Gd-driven actual and nominal CERs, i.e., SI<sub>post</sub>/SI<sub>pre</sub>, were simulated.

### Conversion of SI to Gd-Concentration

MR SI can be converted to the Gd-concentration according to the follow equation:

$$C(t) = (R_1 [t] - R_{1pre}) / r_{1Gd} \quad (6),$$

$$E_{10} = e^{-R_{1pre} \cdot TR} \quad (7),$$

$$B = \frac{1 - E_{10}}{1 - \cos \alpha \cdot E_{10}} \quad (8),$$

$$A = B \cdot CER(t) \quad (9),$$

$$R_1(t) = \frac{-1}{TR} \cdot \ln \left( \frac{1 - A}{1 - \cos \alpha \cdot A} \right) \quad (10),$$

where C(t) = time-dependent Gd-concentration, CER(t) = Gd-driven CER, α = FA, TR = 2.5 msec, and R<sub>1</sub>(t) = time-dependent post-Gd R<sub>1</sub> value. The actual Gd-concentration was calculated by applying the actual values of R<sub>1pre</sub> and CER(t), while the nominal Gd-concentration was calculated using the reference values.

To compare the influence of a deviated pre-contrast R<sub>1</sub> and CER on the Gd-concentration measurement, the variation of Gd-concentration was simulated while using the actual value of one parameter and the reference value of the other.

### AIF

The time-dependent plasma concentration of Gd, i.e., AIF, was calculated using the following equation:

$$C_p(t) = D \cdot \sum_{i=1}^2 a_i \cdot e^{-m_i \cdot t} \quad (11),$$

where C<sub>p</sub>(t) = time-dependent Gd-concentration in the blood, D = the dose of CA (mmole/kg), a<sub>i</sub> = normalized for unit dose (kg/L), and m<sub>i</sub> = rate constant for the plasma curve (min<sup>-1</sup>). The actual a<sub>1</sub>, a<sub>2</sub>, m<sub>1</sub>, and m<sub>2</sub> values were calculated by fitting the actual C<sub>p</sub>(t), while the nominal C<sub>p</sub> was calculated by applying the above-mentioned reference values.

**PK Parameters**

The time-dependent concentration of Gd in the gray matter is described by the following equation:

$$C_t(t) = D \cdot K^{\text{trans}} \sum_{i=1}^2 \left( a_i \cdot \frac{e^{-[K^{\text{trans}}/v_e]t} - e^{-m_i \cdot t}}{m_i - [K^{\text{trans}}/v_e]} \right) + v_p \cdot D \cdot \sum_{i=1}^2 a_i \cdot e^{-m_i \cdot t} \quad (12),$$

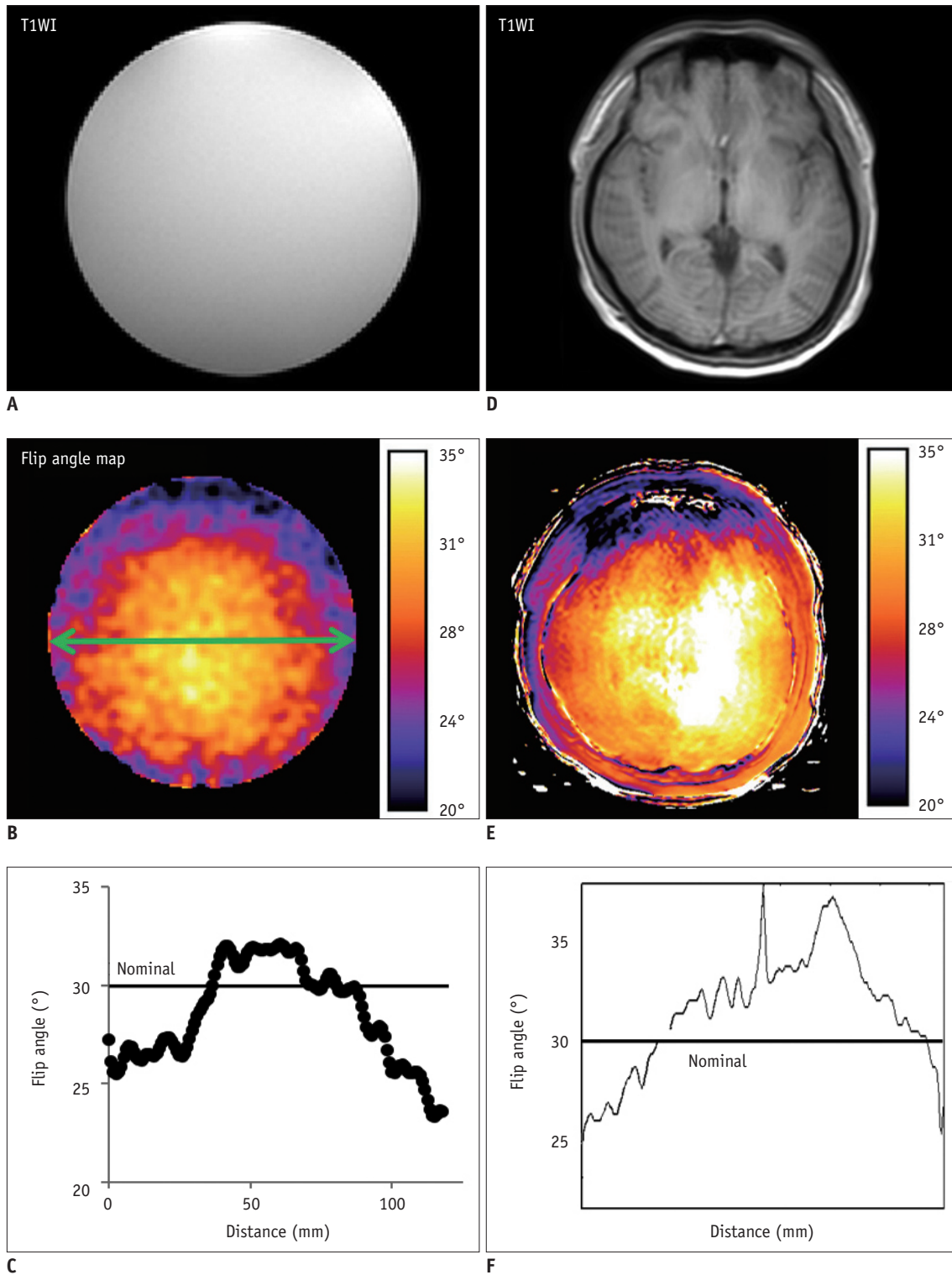


**Fig. 1. Location-dependent distribution of  $B_1$ -inhomogeneity-induced flip angle deviation measured in water phantom (A-C) and normal brain (D-F).** Actual flip angle is greater than nominal flip angle at image center, whereas it was less at periphery. T1WI = T1-weighted image

where  $C_t(t)$  = time-dependent tissue concentration of Gd,  $K^{trans}$  = volume transfer constant between blood and extravascular extracellular space,  $v_e$  = volume of extravascular extracellular space per unit volume of tissue, and  $v_p$  = volume of plasma per unit volume of tissue. The nominal  $C_t(t)$  was generated using the above-mentioned reference values of  $K^{trans}$ ,  $v_e$ , and  $v_p$ , whereas the actual B<sub>1</sub>-error-affected PK parameters were calculated by fitting the actual  $C_t(t)$ .

In order to describe an actual situation of B<sub>1</sub>-inhomogeneity-driven error in PK modeling of DCE-MRI, a sample condition was simulated. With this process, a target lesion in the image center had a 3% FA deviation, and a feeding vessel in the image periphery had a -10% FA deviation. Under this condition, the measurement error occurring in each calculation step, which finally caused a variation of the PK parameters, was computed.

## RESULTS

### Ex Vivo and In Vivo

#### B<sub>1</sub>-Inhomogeneity

The actual FA measured across the phantom and the brain of a normal volunteer is shown in Figure 1. The actual FA demonstrated a location-dependent distribution since it was greater than the nominal FA in the image center, but it was less in the peripheral area. In the phantom, the actual FA corresponding to the nominal FA of 30° was 27.4 ± 2.2° (mean ± SD; range, 23.3–32.1°). The 95% CI of the % error in the actual FA was -23–5% of the nominal FA. In three normal volunteers, the actual FA corresponding to the nominal FA of 30° was 32.5 ± 3.0° (range, 26.7–38.4°) and the 95% CI of the % error as -11–28% of the nominal FA.

**Table 1. Simulation of B<sub>1</sub>-Error-Influenced Deviation**

|   | Gray Matter      | Blood            |
|---|------------------|------------------|
| <b>Precontrast R<sub>1</sub></b>                  |                  |                  |
| Reference value (sec <sup>-1</sup> )              | 0.549            | 0.606            |
| Actual value (sec <sup>-1</sup> )                 |                  |                  |
| Mean ± SD   | 0.674 ± 0.110    | 0.743 ± 0.121    |
| 95% CI  | 0.458–0.889      | 0.505–0.981      |
| Range   | 0.367–1.498      | 0.405–1.652      |
| % error   |                  |                  |
| Mean ± SD   | 22.59 ± 20.02    | 22.59 ± 20.02    |
| 95% CI  | -16.65–61.83     | -16.65–61.82     |
| Range   | -33.19–172.57    | -33.18–172.55    |
| <b>Gd-driven CER</b>                              |                  |                  |
| Difference between actual and nominal values      |                  |                  |
| Mean ± SD   | -0.0105 ± 0.0099 | -0.1881 ± 0.1764 |
| 95% CI  | -0.0298–0.0088   | -0.5339–0.1576   |
| Range   | -0.0464–0.0106   | -1.1615–0.2945   |
| % error   |                  |                  |
| Mean ± SD   | -0.37 ± 0.33     | -1.94 ± 1.66     |
| 95% CI  | -1.02–0.28       | -5.20–1.32       |
| Range   | -1.53–0.35       | -9.06–2.30       |
| <b>Gd-concentration</b>                           |                  |                  |
| Difference between actual and nominal values (mM) |                  |                  |
| Mean ± SD   | 0.0567 ± 0.0513  | 0.3298 ± 0.2897  |
| 95% CI  | -0.0439–0.1573   | -0.2381–0.8976   |
| Range   | -0.0532–0.2377   | -0.3814–1.6963   |
| % error   |                  |                  |
| Mean ± SD   | 21.95 ± 18.45    | 21.85 ± 18.36    |
| 95% CI  | -14.22–58.11     | -14.13–57.82     |
| Range   | -17.48–78.17     | -17.43–77.75     |

CER = contrast-enhancement ratio, Mean ± SD = average and standard deviation values, Range = minimum and maximum values, 95% CI = 95% confidence interval

**Pre-Contrast  $R_1$  Value**

The expected actual FA ranged between 1.54–2.10° for a nominal FA of 2° and 10.8–14.7° for a nominal FA of 14°. By applying 100000 actual FAs within the 95% CI, the  $B_1$ -error-influenced  $R_1$  values showed a variation range as summarized in Table 1 and Figure 2.

Typically, with a -10% FA error, the actual value of 'm' in

Eq-3 measured in the gray matter was 0.9983 whereas its reference value was 0.9986 ( $e^{-R_1 \text{ reference} \cdot TR} = e^{-0.549 \cdot 0.0025}$ ), thereby showing only a -0.03% error. However, according to Eq-4, as the actual  $R_1$  was 0.679  $\text{sec}^{-1}$  ( $\frac{1}{TR} \cdot \ln [\frac{1}{m}] = \frac{1}{0.0025} \cdot \ln [\frac{1}{0.9983}]$ ), the small error of 'm' was increased to a 23.6%  $R_1$  deviation.

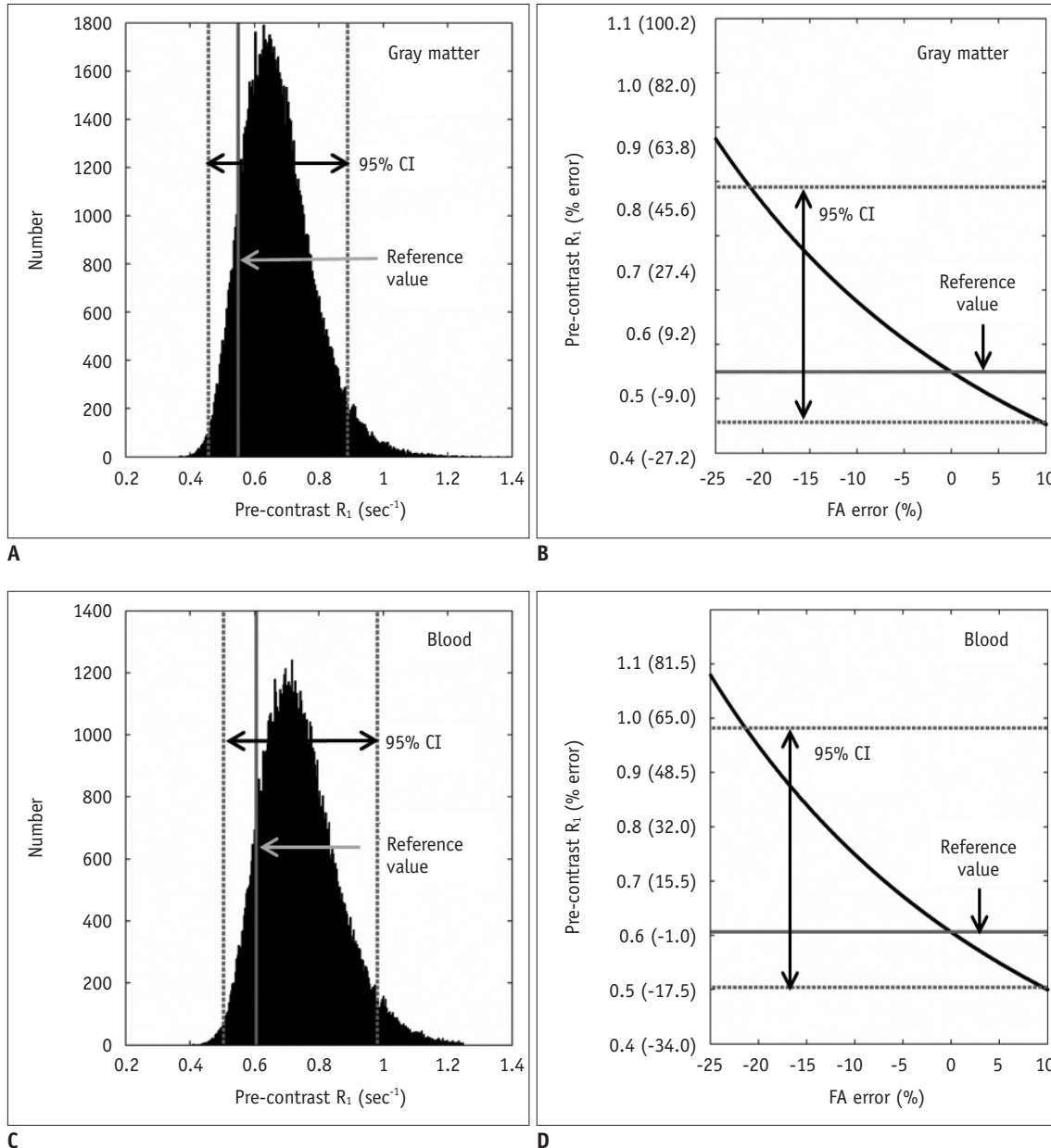


**Fig. 2.**  $B_1$ -inhomogeneity-induced variation of pre-contrast  $R_1$  in gray matter (reference value, 0.549  $\text{sec}^{-1}$ ) and blood (reference value, 0.606  $\text{sec}^{-1}$ ).

**A.** Distribution of actual values of pre-contrast  $R_1$  in gray matter. 95% CI of % error is -16.7–61.8%. **B.** Negative correlation between % error of FA and that of pre-contrast  $R_1$  in gray matter. Actual  $R_1$  is greater than reference value when actual FA was less than nominal FA, and vice versa. **C.** Distribution of actual values of pre-contrast  $R_1$  in blood. 95% CI of % error is -16.7–61.8%. **D.** Negative correlation between % error of FA and that of pre-contrast  $R_1$  in blood. Actual  $R_1$  is greater than reference value when actual FA was less than nominal FA, and vice versa. CI = confidence interval, FA = flip angle

**Gd-Driven CER**

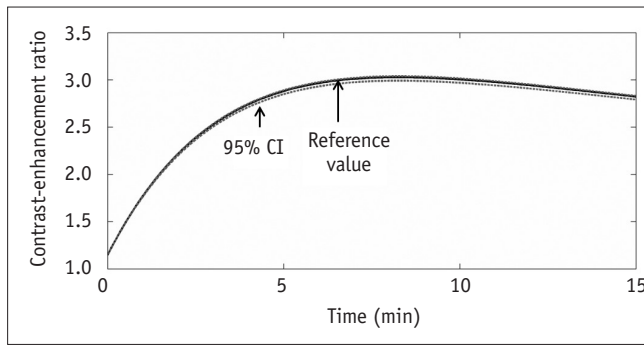
The time-dependent actual Gd-driven CERs are shown in Table 1 and Figure 3. The B<sub>1</sub>-error-induced deviation of CER was not notably high as the 95% CI of % error was only -1.02–0.28% in the gray matter and -5.20–1.32% in the blood. Typically, -10% FA error resulted in -0.400% error in the gray matter and -2.112% error in the blood.

The variation range of the actual CER became greater as the CER increased. For example, the range of the actual CER in the gray matter was 1.38–1.39 (95% CI of % error, -0.32–0.26%) at the nominal CER of 1.4, whereas it was 2.98–3.02 (95% CI of % error, -1.20–0.32%) at the nominal CER of 3.

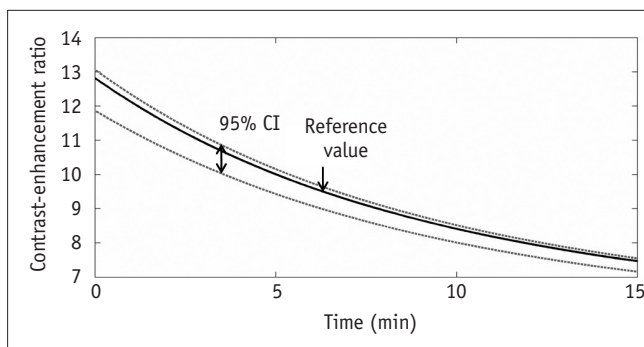
**Gd-Concentration**

The time-dependent actual Gd-concentrations are shown in Table 1 and Figure 4. Characteristically, a -10% FA deviation induced Gd-concentration errors of 23.6% in the gray matter and 23.5% in the blood.

The influence of the R<sub>1</sub> and CER errors on the Gd-



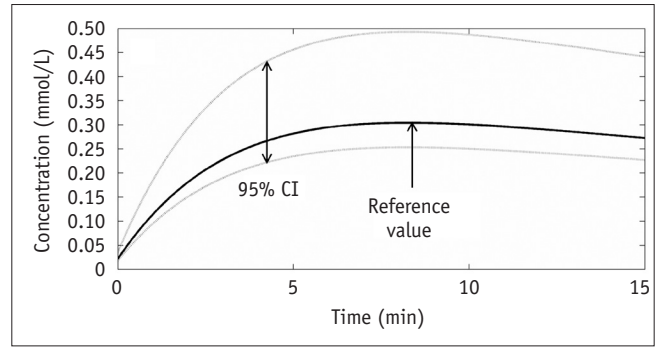
**A**



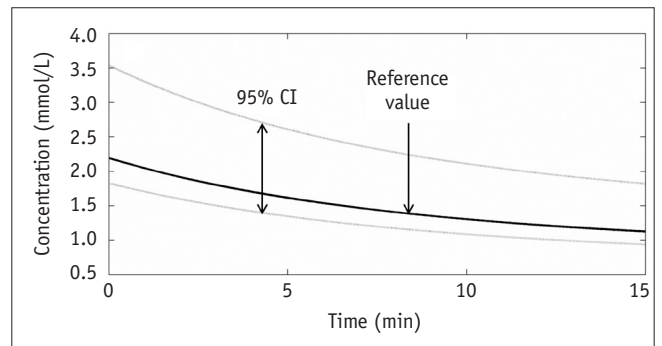
**B**

**Fig. 3. B<sub>1</sub>-inhomogeneity-induced variation of contrast-enhancement ratio in gray matter and blood.**

**A.** Reference and actual curves of time-dependent contrast-enhancement ratio in gray matter. 95% CI of % error is -1.0–0.3%. **B.** Reference and actual curves of time-dependent contrast-enhancement ratio in blood. 95% CI of % error is -5.2–1.3%. CI = confidence interval



**A**



**B**

**Fig. 4. B<sub>1</sub>-inhomogeneity-induced variation of Gd-concentration in gray matter and blood.**

**A.** Reference and actual curves of time-dependent Gd-concentration in gray matter. 95% CI of % error is -14.2–58.1%. **B.** Reference and actual curves of time-dependent Gd-concentration in blood. 95% CI of % error is -14.1–57.8%. CI = confidence interval

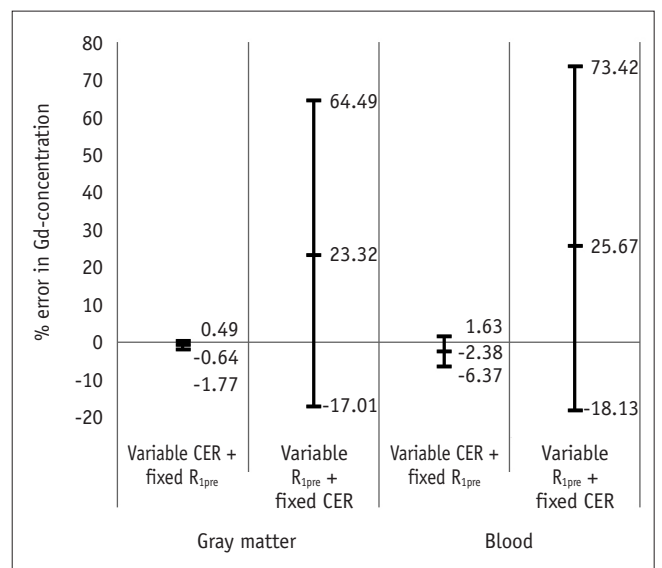


**Fig. 5. Influence of erroneous pre-contrast R<sub>1</sub> and CER on calculation of Gd-concentration.**

Simulation was performed while either of these two parameters was applied as reference value and other as actual value. % error range of Gd-concentration is significantly wider by R<sub>1</sub> error than by CER error. CER = contrast-enhancement ratio, R<sub>1pre</sub> = pre-contrast R<sub>1</sub>

**Table 2. Simulation of Arterial Input Function**

|                 | $a_1$ (kg/L)  | $a_2$ (kg/L)  | $m_1$ (min <sup>-1</sup> ) | $m_2$ (min <sup>-1</sup> ) |
|-----------------|---------------|---------------|----------------------------|----------------------------|
| Reference value | 3.99          | 4.78          | 0.144                      | 0.0111                     |
| Actual value    |               |               |                            |                            |
| Mean ± SD       | 4.88 ± 0.79   | 5.85 ± 0.95   | 0.1438 ± 0.0002            | 0.0111 ± 0.0000            |
| 95% CI          | 3.33–6.44     | 3.99–7.71     | 0.1435–0.1441              | 0.0110–0.0111              |
| Range           | 2.67–10.76    | 3.20–12.89    | 0.1428–0.1444              | 0.0109–0.0112              |
| % error         |               |               |                            |                            |
| Mean ± SD       | 22.40 ± 19.84 | 22.39 ± 19.81 | -0.11 ± 0.11               | -0.26 ± 0.28               |
| 95% CI          | -16.48–61.28  | -16.43–61.22  | -0.32–0.10                 | -0.80–0.28                 |
| Range           | -33.06–169.73 | -33.04–169.66 | -0.82–0.30                 | -1.98–1.09                 |

Mean ± SD = average and standard deviation values, Range = minimum and maximum values, 95% CI = 95% confidence interval

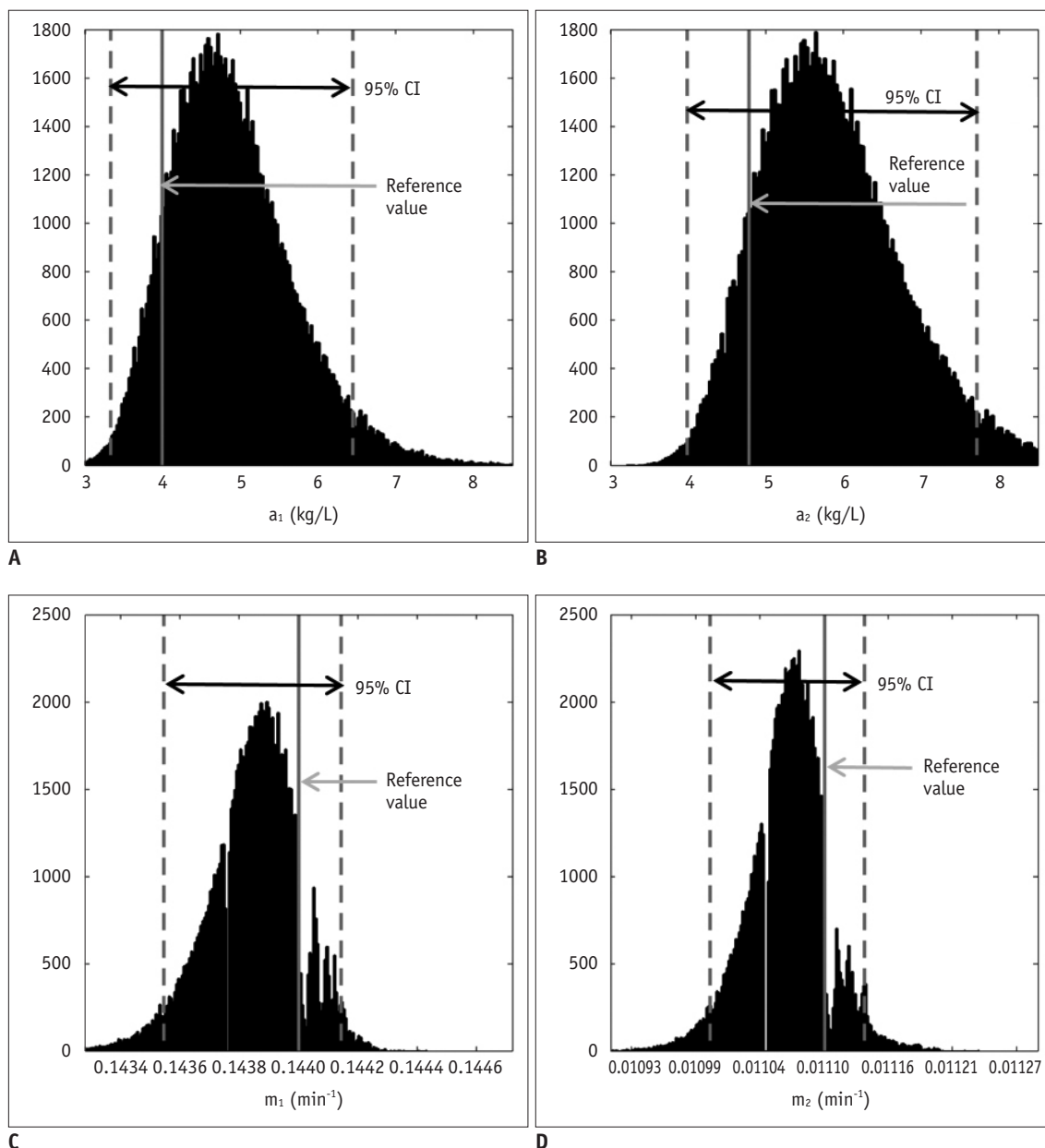


**Fig. 6. B<sub>1</sub>-inhomogeneity-induced variation of four parameters that characterize arterial input function.**

95% CI of % error are -16.5–61.3% for  $a_1$  (A), -16.4–61.2% for  $a_2$  (B), -0.3–0.1% for  $m_1$  (C), and -0.8–0.3% for  $m_2$  (D). CI = confidence interval



concentration is compared in Figure 5, in which either of these two parameters was applied as a reference value and the other as an actual value. This simulation demonstrated that the R<sub>1</sub> error caused a greater variation in the Gd-concentration than in the CER. This is evident from the 95% CI of the Gd-concentration being wider due to the pre-contrast R<sub>1</sub> error than the CER error.

The variation width of the actual Gd-concentration became greater as the Gd-concentration increased. For example, in the gray matter, the 95% CI of actual Gd-concentration was 0.047–0.094 (% error, -19.20–63.33%) at a Gd-concentration of 0.058 mM, whereas it was 0.244–0.493 (% error, -19.17–63.25%) at a Gd-concentration of 0.302 mM.

### AIF

The simulated AIF parameter, calculated by fitting the actual Gd-concentration curve, is presented in Table 2 and Figure 6. Typically, a -10% FA error led to 23.44, 23.43, -0.12, and -0.28% error of a<sub>1</sub>, a<sub>2</sub>, m<sub>1</sub>, and m<sub>2</sub>, respectively. In these simulations, the a<sub>1</sub> and a<sub>2</sub> values which characterize the amplitude of the AIF curve showed a greater FA-dependent variation (95% CI of % error, -16.48–61.28%) than m<sub>1</sub> and m<sub>2</sub> (-0.80–0.28%) which describe the shape of the AIF curve.

### PK Parameters

The distribution of the B<sub>1</sub>-error-influenced PK parameters is shown in Table 3. The 95% CI of % error was -43.1–48.4% in the K<sup>trans</sup>, -43.2–48.6% in the v<sub>e</sub>, and -43.2–48.6% in the v<sub>p</sub>. Characteristically, a -10% FA error led to 17.51% error in the K<sup>trans</sup>, 17.49% in the v<sub>e</sub>, and 17.58% in the v<sub>p</sub>.

All of these parameters demonstrated a negative correlation with the % error of FA in that they were higher than the reference values when the actual FA was lower

than the nominal FA.

### Simulation Example

According to the simulation example, in which the FA error is 3% in a target lesion and -10% in a feeding vessel, the % error of the PK parameter was -23.66% for the K<sup>trans</sup>, -23.71% for the v<sub>e</sub>, and -23.70% for the v<sub>p</sub>. Detailed results are given in Figure 7.

## DISCUSSION

This study analyzed the influence of B<sub>1</sub>-inhomogeneity on the PK modeling of DCE-MRI. In the phantom experiment on a 3T unit that undergoes regular vendor-guided equipment maintenance, a considerable range was observed in the actual FA (95% CI, -23–5%) with a nominal FA of 30°. Subsequently, Monte Carlo simulation using a similar FA variation demonstrated that the B<sub>1</sub>-inhomogeneity-induced incorrect measurement of pre-contrast R<sub>1</sub> (-17–62%) as well as the Gd-driven CER (-5–1%) led to a substantial deviation of the Gd-concentration (-14–58%). Finally, our simulation demonstrated a significant variation in the PK parameters (-43–49%), which would be beyond a tolerable error range in clinical practice (16).

According to our simulation, the FA variation has a greater effect on the pre-contrast R<sub>1</sub> measurement than on the CER. In this respect, a -10% FA deviation caused a 23.6% R<sub>1</sub> error but only a -0.4% CER error in the gray matter. We suggest that this strong vulnerability of the pre-contrast R<sub>1</sub> to FA inhomogeneity is closely related to the calculation process in the VFA method. According to the Eq-4 and TR of 5 msec,  $R_1 = \frac{1}{TR} \cdot \ln\left(\frac{1}{m}\right) = \frac{1}{0.0025} \cdot \ln\left(\frac{1}{m}\right) = 400 \cdot \ln\left(\frac{1}{m}\right)$ . As such, multiplication of  $\frac{1}{TR}$ , i.e., 400, amplifies a small variation of 'm' to a substantial error of R<sub>1</sub>. For example in our simulation, only a -0.03% deviation of 'm' led to

**Table 3. Simulation of Pharmacokinetic Parameters**

|                 | K <sup>trans</sup> (min <sup>-1</sup> ) | v <sub>e</sub>  | v <sub>p</sub>  |
|-----------------|---|-----------------|-----------------|
| Reference value | 0.05                                    | 0.21            | 0.010           |
| Actual value    |   |                 |                 |
| Mean ± SD       | 0.0513 ± 0.0117                         | 0.2155 ± 0.0491 | 0.0103 ± 0.0023 |
| 95% CI          | 0.0285–0.0742                           | 0.1193–0.3117   | 0.0057–0.0149   |
| Range           | 0.0196–0.1310                           | 0.0820–0.5504   | 0.0039–0.0263   |
| % error         |   |                 |                 |
| Mean ± SD       | 2.67 ± 23.35                            | 2.62 ± 23.43    | 2.71 ± 23.43    |
| 95% CI          | -43.10–48.44                            | -43.22–48.64    | -43.22–48.64    |
| Range           | -60.83–162.00                           | -60.94–163.03   | -60.94–163.03   |

Mean ± SD = average and standard deviation values, Range = minimum and maximum values, 95% CI = 95% confidence interval

a 23.6% error of  $R_1$ . Moreover, as the pre-contrast  $R_1$  is used from the first step in converting the DCE-MRI SI to the Gd-concentration, its deviation continuously affects the subsequent calculations in the PK modeling. As shown in our simulation example, a 23.6% deviation of blood pre-contrast  $R_1$ , which was induced by a -10% FA error, ultimately causes approximately -24% deviations of  $K^{trans}$ ,  $v_e$ , and  $v_p$ . Therefore, in order to improve the accuracy and reliability of PK parameter measurements, it is necessary to control the propagation of  $R_1$  error throughout a number of

steps in the Gd-concentration estimation.

In order to reduce the undesirable effect of  $B_1$ -inhomogeneity on estimation of PK parameters, the application of  $B_1$ -corrected  $R_1$  mapping is the primary recommended solution (20, 21). In a recent study the  $B_1$  field was accurately homogenized by a linear, inverse, distant-weighted interpolation. This study demonstrated that this  $B_1$  correction could reduce the difference in the *in vivo*  $T_1$  value, between the inversion recovery and VFA methods, from 58% to 8.1% in the breast coil

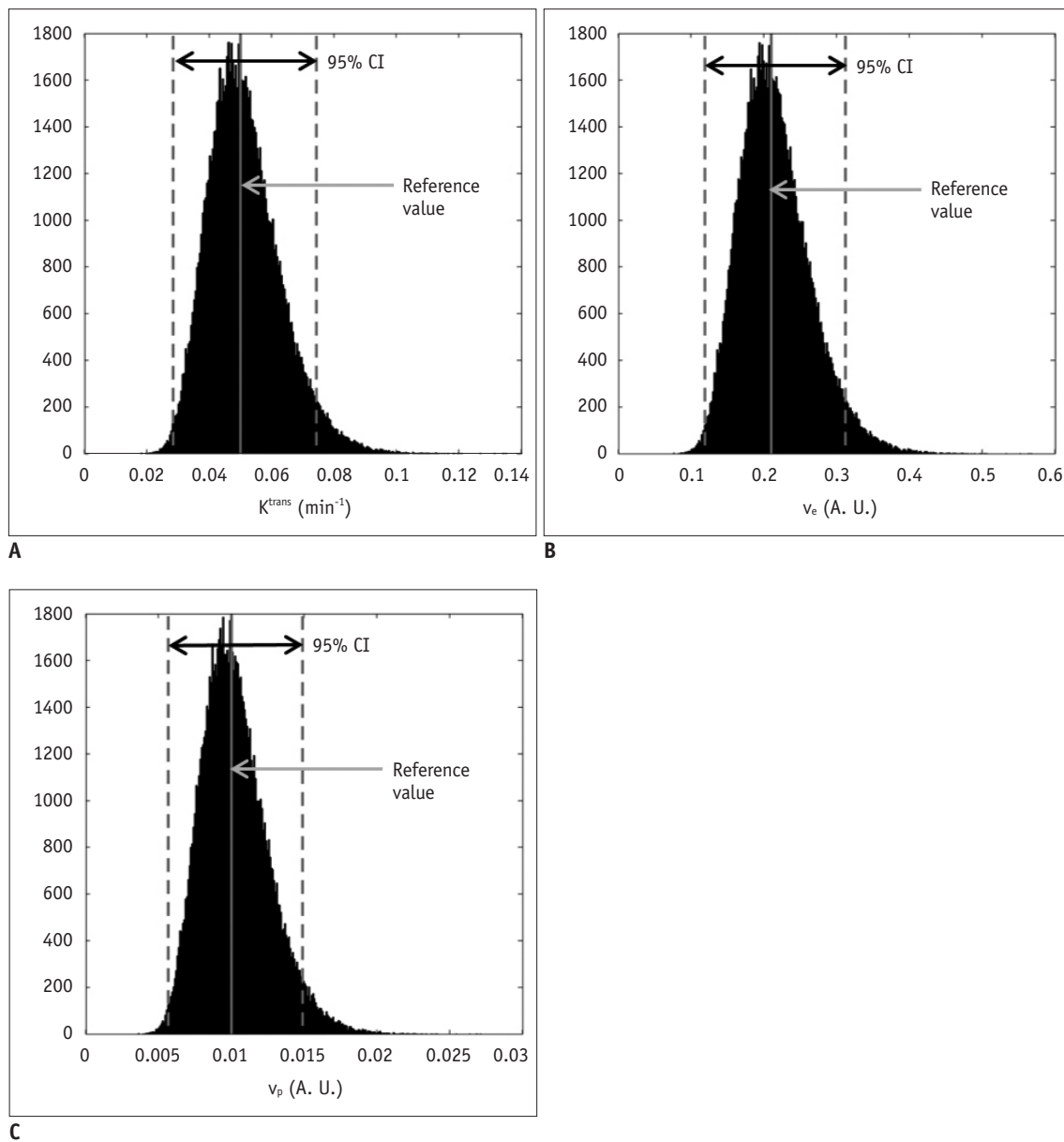


**Fig. 7.** Example case that simulates actual situation reflecting influence of  $B_1$ -inhomogeneity on pharmacokinetic modeling of DCE-MRI. In this simulation, target lesion in image center has 3% FA deviation and feeding vessel in image periphery has -10% FA deviation, which leads to measurement error occurring in each calculation step of pharmacokinetic modeling. Finally, % errors for pharmacokinetic parameters were -23.7% for  $K^{trans}$  (A), -23.7% for  $v_e$  (B), and -23.7% for  $v_p$  (C). A. U. = arbitrary unit, CI = confidence interval, DCE-MRI = dynamic contrast-enhanced magnetic resonance imaging

(21). According to Eq-3 and -4, such an 8.1% R<sub>1</sub> error is approximately equivalent to an FA error of 4%. Therefore, the B<sub>1</sub> correction can reduce not only the R<sub>1</sub> deviation but also the CER error, thereby significantly improving the quality of PK modeling.

Applying a long TR in a condition that satisfies the acceptable scanning time can be another solution for reducing the variation of pre-contrast R<sub>1</sub>. Our simulation used a TR of 2.5 msec for the VFA method as recommended by the QIBA guidelines when using the same pulse sequence for R<sub>1</sub> measurement as used for the DCE-MRI (16). However, as detailed in Eq-4, the use of a longer TR can reduce the effect of deviated 'm' while not disturbing the PK modeling. For example, a TR of 5 msec may reduce the effect of deviated 'ln (1 / m)' by half compared with a TR of 2.5 msec.

A majority of two-compartment models analyze the shape of the time-concentration curve, and therefore are strongly dependent on the accuracy of the Gd-concentration. Therefore, these methods are inherently affected by the FA-dependent error, as described above. On the other hand, an algorithm that was initially proposed by Brix et al. (22) and then modified by Hoffmann et al. (23) estimates PK parameters directly from the DCE-MRI SI. Therefore, this method has an important advantage to avoid potential errors occurring during the measurement of pre-contrast R<sub>1</sub> and Gd-concentration. The feasibility of this simple approach as an alternative to the complex, two-compartment models has been validated in several clinical trials (22, 24-26). Another benefit of this method is that there is no requirement for AIF measurement which has been seriously considered as a major error source in PK modeling (27). However, the usage of this algorithm is acceptable only under specific permeability-limiting conditions (17, 28), and does not provide the blood volume. Therefore, a larger-scale verification regarding its strength and weakness is necessary, which must be based on a comparison with the concentration-based, two-compartment models.

In the present study, the B<sub>1</sub>-inhomogeneity was measured using a brain coil. As the B<sub>1</sub>-inhomogeneity increases in a larger field of view, the FA variation must be greater in the body and breast coils than in the brain coil. Actually, previous breast coil studies showed a wider deviation of FA (median, -40%; and greater than -50% in some cases) than this study (7, 10). Consequently, the variation of FA and the subsequent measurement error of PK parameters may be augmented when using the breast or body coil.

The influence of B<sub>1</sub>-inhomogeneity on PK parameter

estimation from DCE-MRI was also simulated by Di Giovanni et al. (9) who showed a greater variation of the PK parameters than that seen in our study (for example, K<sup>trans</sup> and v<sub>e</sub> error up to 531% and 233%). For the simulation, they separately employed the deviated pre-contrast R<sub>1</sub> and FA for DCE-MRI, which referred to the values seen in the literature reports. In contrast, our simulation applied such parameters originating from a single B<sub>1</sub>-inhomogeneity condition on the basis of a phantom experiment, and therefore may be more realistic for predicting an error occurring in each MRI unit. Moreover, again comparing with Di Giovanni et al. (9), this simulation included the deviation of AIF induced by FA error, and used the modified Tofts model that measures the v<sub>p</sub>. Although the etiology and phenomenon of unstable PK modeling are similarly considered, the dissimilar simulation setting seems to be the main cause of such different error ranges in the PK parameters from different studies.

In conclusion, this study demonstrates the influences of B<sub>1</sub>-inhomogeneity on PK parameter estimation using DCE-MRI. An understanding of the inherent FA error, which occurs even in clinically utilized MR units and its impact on PK modeling, will help to establish strategies for using DCE-MRI to improve the quantification of disease- or treatment-driven vascular alterations.

## REFERENCES

1. Li SP, Padhani AR. Tumor response assessments with diffusion and perfusion MRI. *J Magn Reson Imaging* 2012;35:745-763
2. Jahng GH, Li KL, Ostergaard L, Calamante F. Perfusion magnetic resonance imaging: a comprehensive update on principles and techniques. *Korean J Radiol* 2014;15:554-577
3. Paik W, Kim HS, Choi CG, Kim SJ. Pre-operative perfusion skewness and kurtosis are potential predictors of progression-free survival after partial resection of newly diagnosed glioblastoma. *Korean J Radiol* 2016;17:117-126
4. Wang CH, Yin FF, Horton J, Chang Z. Review of treatment assessment using DCE-MRI in breast cancer radiation therapy. *World J Methodol* 2014;4:46-58
5. van Schie JJ, Lavini C, van Vliet LJ, Vos FM. Feasibility of a fast method for B1-inhomogeneity correction for FSPGR sequences. *Magn Reson Imaging* 2015;33:312-318
6. Tofts PS, Brix G, Buckley DL, Evelhoch JL, Henderson E, Knopp MV, et al. Estimating kinetic parameters from dynamic contrast-enhanced T(1)-weighted MRI of a diffusable tracer: standardized quantities and symbols. *J Magn Reson Imaging* 1999;10:223-232
7. Azlan CA, Di Giovanni P, Ahearn TS, Semple SI, Gilbert FJ, Redpath TW. B1 transmission-field inhomogeneity and enhancement ratio errors in dynamic contrast-enhanced

- MRI (DCE-MRI) of the breast at 3T. *J Magn Reson Imaging* 2010;31:234-239
8. Dietrich O, Reiser MF, Schoenberg SO. Artifacts in 3-T MRI: physical background and reduction strategies. *Eur J Radiol* 2008;65:29-35
  9. Di Giovanni P, Azlan CA, Ahearn TS, Semple SI, Gilbert FJ, Redpath TW. The accuracy of pharmacokinetic parameter measurement in DCE-MRI of the breast at 3 T. *Phys Med Biol* 2010;55:121-132
  10. Kuhl CK, Kooijman H, Gieseke J, Schild HH. Effect of B1 inhomogeneity on breast MR imaging at 3.0 T. *Radiology* 2007;244:929-930
  11. Sung K, Daniel BL, Hargreaves BA. Transmit B1+ field inhomogeneity and T1 estimation errors in breast DCE-MRI at 3 tesla. *J Magn Reson Imaging* 2013;38:454-459
  12. Yarnykh VL. Actual flip-angle imaging in the pulsed steady state: a method for rapid three-dimensional mapping of the transmitted radiofrequency field. *Magn Reson Med* 2007;57:192-200
  13. Ahearn TS, Staff RT, Redpath TW, Semple SI. The use of the Levenberg-Marquardt curve-fitting algorithm in pharmacokinetic modelling of DCE-MRI data. *Phys Med Biol* 2005;50:N85-N92
  14. Deoni SC. High-resolution T1 mapping of the brain at 3T with driven equilibrium single pulse observation of T1 with high-speed incorporation of RF field inhomogeneities (DESPOT1-HIFI). *J Magn Reson Imaging* 2007;26:1106-1111
  15. Schabel MC, Morrell GR. Uncertainty in T(1) mapping using the variable flip angle method with two flip angles. *Phys Med Biol* 2009;54:N1-N8
  16. Quantitative Imaging Biomarkers Alliance. Profile: DCE MRI Quantification. Available at: [http://qibawiki.rsna.org/images/7/7b/DCEMRIProfile\\_v1\\_6-20111213.pdf](http://qibawiki.rsna.org/images/7/7b/DCEMRIProfile_v1_6-20111213.pdf). Accessed December 23, 2015
  17. Khalifa F, Soliman A, El-Baz A, Abou El-Ghar M, El-Diasty T, Gimelfarb G, et al. Models and methods for analyzing DCE-MRI: a review. *Med Phys* 2014;41:124301
  18. Weissleder R, Cheng HC, Marecos E, Kwong K, Bogdanov A Jr. Non-invasive in vivo mapping of tumour vascular and interstitial volume fractions. *Eur J Cancer* 1998;34:1448-1454
  19. Tofts PS. Modeling tracer kinetics in dynamic Gd-DTPA MR imaging. *J Magn Reson Imaging* 1997;7:91-101
  20. Willinek WA, Gieseke J, Kukuk GM, Nelles M, König R, Morakkabati-Spitz N, et al. Dual-source parallel radiofrequency excitation body MR imaging compared with standard MR imaging at 3.0 T: initial clinical experience. *Radiology* 2010;256:966-975
  21. Pineda FD, Medved M, Fan X, Karczmar GS. B1 and T1 mapping of the breast with a reference tissue method. *Magn Reson Med* 2016;75:1565-1573
  22. Brix G, Semmler W, Port R, Schad LR, Layer G, Lorenz WJ. Pharmacokinetic parameters in CNS Gd-DTPA enhanced MR imaging. *J Comput Assist Tomogr* 1991;15:621-628
  23. Hoffmann U, Brix G, Knopp MV, Hess T, Lorenz WJ. Pharmacokinetic mapping of the breast: a new method for dynamic MR mammography. *Magn Reson Med* 1995;33:506-514
  24. Scharf J, Kemmling A, Hess T, Mehrabi A, Kauffmann G, Groden C, et al. Assessment of hepatic perfusion in transplanted livers by pharmacokinetic analysis of dynamic magnetic resonance measurements. *Invest Radiol* 2007;42:224-229
  25. Ma HT, Griffith JF, Yeung DK, Leung PC. Modified brix model analysis of bone perfusion in subjects of varying bone mineral density. *J Magn Reson Imaging* 2010;31:1169-1175
  26. Kiessling F, Lichy M, Grobholz R, Heilmann M, Farhan N, Michel MS, et al. Simple models improve the discrimination of prostate cancers from the peripheral gland by T1-weighted dynamic MRI. *Eur Radiol* 2004;14:1793-1801
  27. Sung YS, Park B, Choi Y, Lim HS, Woo DC, Kim KW, et al. Dynamic contrast-enhanced MRI for oncology drug development. *J Magn Reson Imaging* 2016;44:251-264
  28. Brix G, Griebel J, Kiessling F, Wenz F. Tracer kinetic modelling of tumour angiogenesis based on dynamic contrast-enhanced CT and MRI measurements. *Eur J Nucl Med Mol Imaging* 2010;37 Suppl 1:S30-S51